DOI: 10.1093/brain/awg089 *Brain* (2003), **126,** 974–987

Central nervous system inflammation is a hallmark of pathogenesis in mouse models of GM1 and GM2 gangliosidosis

M. Jeyakumar,[1] R. Thomas,[1] E. Elliot-Smith,[1] D. A. Smith,[1] A. C. van der Spoel,[1] A. d'Azzo,[3] V. Hugh Perry,[2] T. D. Butters,[1] R. A. Dwek[1] and F. M. Platt[1]

[1]*Glycobiology Institute, Department of Biochemistry, University of Oxford, Oxford,* [2]*CNS Inflammation Group, School of Biological Sciences, University of Southampton, Southampton, UK,* [3]*Department of Genetics, St Jude Children's Hospital, Memphis, TN, USA*

Correspondence to: Dr Frances M. Platt, Department of Biochemistry, University of Oxford, South Parks Road, Oxford OX1 3QU, UK
E-mail: fran@glycob.ox.ac.uk

Summary

Mouse models of the GM2 gangliosidoses [Tay-Sachs, late onset Tay-Sachs (LOTS), Sandhoff] and GM1 gangliosidosis have been studied to determine whether there is a common neuro-inflammatory component to these disorders. During the disease course, we have: (i) examined the expression of a number of inflammatory markers in the CNS, including MHC class II, CD68, CD11b (CR3), 7/4, F4/80, nitrotyrosine, CD4 and CD8; (ii) profiled cytokine production [tumour necrosis factor α (TNFα), transforming growth factor (TGFβ1) and interleukin 1β (IL1β)]; and (iii) studied blood-brain barrier (BBB) integrity. The kinetics of apoptosis and the expression of Fas and TNF-R1 were also assessed. In all symptomatic mouse models, a progressive increase in local microglial activation/expansion and infiltration of inflammatory cells was noted. Altered BBB permeability was evident in Sandhoff and GM1 mice, but absent in LOTS mice. Progressive CNS inflammation coincided with the onset of clinical signs in these mouse models. Substrate reduction therapy in the Sandhoff mouse model slowed the rate of accumulation of glycosphingolipids in the CNS, thus delaying the onset of the inflammatory process and disease pathogenesis. These data suggest that inflammation may play an important role in the pathogenesis of the gangliosidoses.

Keywords: CNS inflammation; gangliosidosis; microglia; pathogenesis; therapy

Abbreviations: BBB = blood-brain barrier; BMT = bone marrow transplantation; GSL = glycosphingolipid; IL1β = interleukin 1β; iNOS = inducible nitric oxide synthase; LOTS = late onset Tay-Sachs; Mϕ = macrophages; *N*B-DNJ = *n*-butyldeoxynojirimycin; NITT = nitrotyrosine; SH = Sandhoff disease; SRT = substrate reduction therapy; TGFβ1 = transforming growth factor; TNFα = tumour necrosis factor α; TUNEL = terminal deoxynucleotide transferase-mediated dUTP nick end labelling

Introduction

The glycosphingolipid (GSL) lysosomal storage diseases are inherited metabolic diseases in which a gene encoding a lysosomal hydrolase or one of their co-factors is mutated. This results in either the total loss of enzyme activity or the retention of some residual enzyme activity, depending on the nature of the specific mutation. The GSL substrate for the deficient enzyme progressively accumulates in the lysosome. Clinical presentation of disease occurs either in infancy (little or no residual enzyme), childhood (low levels of residual enzyme) or adolescence/adulthood (moderate levels of residual enzyme activity). The latter disease variant is termed chronic or late onset. The majority of these disorders are inherited in an autosomal recessive fashion with heterozygotes unaffected, indicating that 50% residual enzyme is sufficient to escape disease.

Two main classes of GSL storage diseases occur, those in which the storage GSL is a neutral GSL species (Gaucher and Fabry diseases) and the gangliosidoses in which the storage lipid is a ganglioside (GSL containing one or more sialic acid residue). The gangliosidoses include the GM2 storage disorders, Tay-Sachs (TS) and Sandhoff (SH) disease, and the GM1 storage disorder termed GM1 gangliosidosis. Gangliosides are expressed abundantly in the nervous system and so the gangliosidoses are characterized by a progressive

Table 1 *Mice used for biochemical and histological analysis*

Mice	Symptoms onset (months)	Average life span, months (*n*)	Age range analysed (months)
Sandhoff ($Hexb^{-/-}$)	~2.5	~4.5 (38)	0.1–4.5
Sandhoff ($Hexb^{-/-}$) *N*B-DNJ*	~3.5	~6 (22)	4–6
Sandhoff ($Hexb^{-/-}$) BMT**	~4	~7.5 (12)	4–7
GM1 gangliosidosis ($\beta Gal^{-/-}$)	~4–5.5	~10 (20)	1–10.3
LOTS ($Hexa^{-/-}$)	~12–18	~20 (12)	16–24
Tay-Sachs ($Hexa^{-/-}$)	None	~30 (18)	1–25
Wild type	None	~30 (15)	1–28

*2400 mg/kg per day from 1.5 months of age (Jeyakumar *et al*., 1999); **transplanted when mice were 10 days old (Norflus *et al*., 1998).

neurodegenerative course. The genetic lesion, resulting enzyme deficiency and the nature of the storage lipid have been well characterized for all the GSL storage disorders, but we currently do not understand how storage leads to pathology.

The development of rational treatments for complex neurodegenerative diseases such as the gangliosidoses will require a detailed knowledge of the underlying mechanisms of disease pathogenesis. With the recent development of authentic animal models (Yamanaka *et al*., 1994; Taniike *et al*., 1995; Phaneuf *et al*., 1996; Sango *et al*., 1996; Hahn *et al*., 1997; Liu *et al*., 1997; Suzuki *et al*., 1997; Tifft and Proia, 1997), a question that can now be asked is: by what mechanisms can lysosomal storage bring about damage to the CNS and brain dysfunction?

Some possible explanations for the pathogenesis of the gangliosidoses have been proposed, none of which are mutually exclusive. For example, abnormal accumulation of GSLs and their metabolites could directly cause neurotoxicity (Suzuki, 1998). Meganeurites and ectopic dendrites characteristic of the gangliosidoses could lead to the onset and progression of neuronal dysfunction by altering electrical properties of the neurone (Walkley, 1998). Also, inappropriate apoptosis of neurones caused by accumulation of GSLs could either directly or indirectly trigger the pathways of programmed cell death (Huang *et al*., 1997; Walkley, 1998).

However, a factor that has only recently been investigated in the genesis of neuronal dysfunction is inflammation (Wada *et al*., 2000). In the CNS of a Sandhoff disease mouse model and in a Sandhoff disease human autopsy, macrophage/microglial activation was detected, implicating a neuroinflammatory component in this disorder. What was unclear from this study was whether this is a general feature of the gangliosidoses or a specific response to the storage of GM2 ganglioside.

To understand the disease process in the gangliosidoses better, we have looked for evidence of CNS immune activation in mouse models of Tay-Sachs, late onset Tay-Sachs (LOTS) and Sandhoff diseases, all of which store GM2 ganglioside but to differing degrees (SH > LOTS > TS). The Tay-Sachs mice are asymptomatic (Yamanaka *et al*., 1994; Taniike *et al*., 1995), the LOTS mice develop chronic disease (Jeyakumar *et al*., 2002*b*) and the Sandhoff mice have an acute rapidly progressive neurodegenerative course (Sango *et al*., 1995; Phaneuf *et al*., 1996; Suzuki *et al*., 1997). This allows the relationship between degree of inflammation, storage levels and pathology to be correlated. However, we have also extended our study to a mouse model of GM1 gangliosidosis as this will allow us to determine whether inflammation in the CNS of GM2 gangliosidosis mouse models is storage lipid-specific or a general response to ganglioside storage.

We have established the kinetics of the inflammatory process and found it to be common to all symptomatic mouse models of GM1 and GM2 storage evaluated. Inflammation pre-dates symptom onset in the symptomatic models studied, suggesting a potentially contributory role in disease progression. In parallel, ganglioside storage, cytokine production, blood-brain barrier (BBB) integrity and the kinetics of apoptosis were also studied to correlate clinical disease stages with pathological events. When an effective therapy for GSL storage diseases [substrate reduction therapy (SRT)] was evaluated in Sandhoff mice, the treated animals showed marked reductions in inflammation, consistent with inflammation playing a role in disease pathogenesis.

Material and methods

Mice

Tay-Sachs ($Hexa^{-/-}$) and Sandhoff ($Hexb^{-/-}$) mice (Yamanaka *et al*., 1994; Sango *et al*., 1995; Taniike *et al*., 1995; Phaneuf *et al*., 1996) were provided by Dr Richard Proia (National Institutes of Health, Bethesda, MD, USA). LOTS mice were generated by repeated breeding of female Tay-Sachs mice, as described previously (Jeyakumar *et al*., 2002*b*). GM1 gangliosidosis mice ($\beta gal^{-/-}$) were provided by Dr Alessandra d'Azzo (St Jude Children's Hospital, Memphis, TN, USA) (Hahn *et al*., 1997). All mice were bred and housed under standard non-sterile conditions, with food and water available ad lib. All animal studies were conducted using protocols approved by the UK Home Office licence (Animals Scientific Procedures Act, 1986). Mice used for this study are

Table 2 *Primary antibodies used for immunohistochemistry*

Antigen	Expression (Gordon *et al.*, 1992; Granville *et al.*, 1998)	Antibody	Source
MHC class II	Activated macrophage (Mϕ)/microglial cells	Rat anti-mouse MHC II	Serotec, Oxford, UK
TNF-R1	Tumour necrosis factor receptor type 1; mediator of apoptosis	Goat anti-TNF-R1 (G-20)	Santa Cruz, California, USA
Fas (APO1; CD95)	Cell surface antigen on activated T- and B-lymphocytes; mediator of apoptosis	Rabbit anti-Fas (Ab-1)	Oncogene, Nottingham, UK
F4/80	Mϕ specific plasma membrane differentiation antigen; expressed by Mϕ/microglial cells	Rat anti-mouse F4/80	Serotec
CD68	Predominantly lysosomal antigen in Mϕ	Rat anti-mouse CD68	Serotec
CR3 (CD11b)	Complement receptor type 3; expressed in polymorphonuclear cells, Mϕ and NK cells	Rat anti-mouse CD11b	Serotec
7/4	Polymorphonuclear cells and activated Mϕ/microglial cells	Rat anti-mouse 7/4	Serotec
CD4	Helper T-cell marker	Rat anti-mouse CD4	Serotec
CD8	Cytotoxic T-cell marker	Rat anti-mouse CD8	Serotec
Nitrotyrosine (NITT)	Stable end product of peroxynitrite oxidation; formed in the presence of the active metabolite NO	Rabbit anti-nitrotyrosine	Chemicon, Harrow, UK
iNOS	Inducible nitric oxide synthase	Rabbit anti-iNOS	Chemicon
NeuN	Neurone-specific nuclear protein; neuronal nuclei	Mouse anti-NeuN	Chemicon
GFAP	Glial fibrillary acidic protein in astrocytes	Mouse anti-GFAP	Sigma, Dorset, UK

summarized in Table 1. Drug treatment (Platt *et al*., 1997) and bone marrow transplantation (BMT) (Norflus *et al*., 1998) were carried out as described previously. *n*-butyldeoxynojirimycin (*N*B-DNJ) was a gift from Searle/Monsanto and Oxford GlycoSciences.

Tissue processing

Mice were killed by CO_2 asphyxiation and were immediately dissected. Brain and spinal cord (cervical C1–C3 region) were freeze-embedded in OCT embedding medium (BDH, Dorset, UK). For perfusion fixed tissues, the mouse was lethally anaesthetized (Hypnorm/Hypnovel i.p.). Transcardiac perfusion was initiated with 50 ml of heparinized saline, followed by 100 ml of PLP fixative (2% paraformaldehyde, lysine, periodate in 0.1 M phosphate buffer pH 6.8) (McLean and Nakane, 1974). The tissues were removed and placed in fixative for 4–6 h at 4°C, transferred to 20% sucrose in 0.1 M phosphate buffer pH 7.2 overnight at 4°C, and freeze-embedded in OCT as described above. Cryostat sections (10 μm) at 1 in 20 intervals were collected onto glass microscope slides, air dried for 4–6 h and stored at –70°C.

Histology

Periodic acid-Schiff reagent and electron microscopy

Periodic acid-Schiff (PAS) reagent and electron microscopy were performed as described previously (Jeyakumar *et al*., 1999).

Histochemistry

The staining method was based on the avidin-biotin peroxidase complex (ABC) technique of Hsu and colleagues (Hsu *et al*., 1981). Basic staining procedures for antibodies and lectins were adapted from Perry *et al*. (1985) and Mannoji *et al*. (1986), respectively. For age-dependent analysis of neuro-inflammation, all age-point sections were processed simultaneously. The sections were incubated in a humid chamber at room temperature for 1–2 h with one of the following primary antibodies (Table 2).

The primary antibodies were detected using one of the following species-specific secondary antibodies: biotinylated rabbit anti-rat immunoglobulin G (IgG; Vector Laboratories, Peterborough, UK), biotinylated mouse anti-rabbit IgG (Sigma), biotinylated rabbit anti-goat (Vector Laboratories), biotinylated horse anti-mouse IgG, and Fluorescein or Texas Red horse anti-mouse (Vector Laboratories). The secondary (biotinylated) antibodies were detected using ABC kit (Vectastain™) and developed with 3.3′-diaminobenzidine (DAB). In control incubation, the primary antibody was replaced by an appropriate non-immune IgG to verify the specificity of staining.

For lectin staining, sections were incubated with either RCA_{120} [biotinylated, β-D-galactosyl-specific, predominantly reacting with activated microglia/macrophages (Mϕ)] or GSL

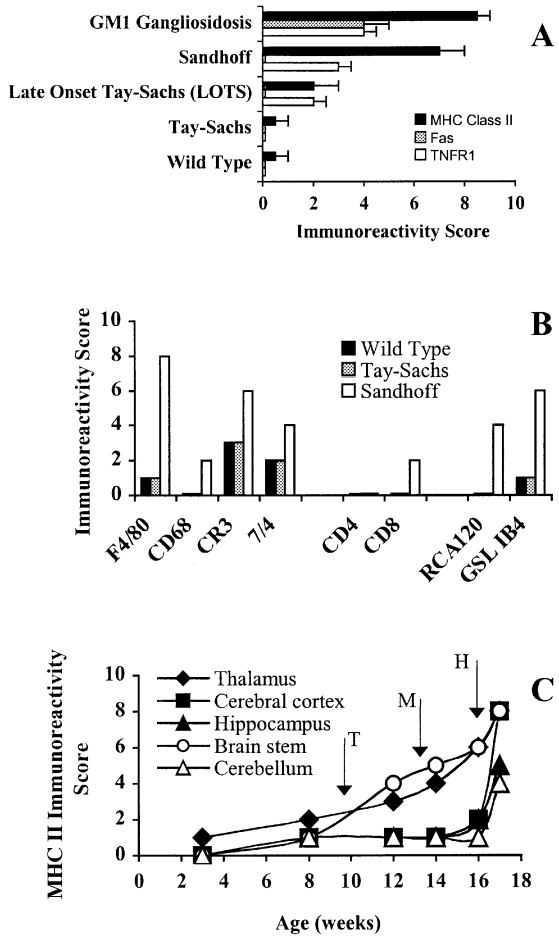

Fig. 1 Inflammatory marker expression in mouse brains. (**A**) MHC class II, Fas and TNF-R1 expression in late disease stage brains (GM1 mice, ~10 months; Sandhoff mice, ~17 weeks; LOTS mice, ~20 months) compared with the asymptomatic Tay-Sachs or wild-type mice (~17 weeks). Data are mean ± SD of the values based on at least three animals in each group. (**B**) Distribution of inflammatory markers throughout the brain in late-stage Sandhoff mice (~17 weeks) compared with age-matched Tay-Sachs and wild type. (**C**) Time course of MHC class II expression in Sandhoff mouse brain. T = head tremor; M = motor dysfunction; H = hind limb paralysis. The data in **B** and **C** are based on two animals per group and the variation of the immunoreactivity score, measured by the SD, was always at least five times smaller than the magnitude of the mean values.

I-B_4 (biotinylated, α-D-galactosyl-specific, reacting with activated and resident microglia/Mϕ) at a concentration of 10 μg/ml in 0.01 M Tris–HCl buffer (with 0.1 mM $CaCl_2$ and 0.01 mM $MgCl_2$, pH 7.4). They were processed according to the ABC method using ABC kit (Vectastain™), and developed with DAB.

Measurement of cytokines

Brains were rapidly removed without meninges, snap frozen in liquid nitrogen and stored at –70°C. The tissue was homogenized on ice in phosphate-buffered saline (PBS; ~0.1 g/ml) containing protease inhibitors (Protease inhibitor Cocktail Set III; Calbiochem, California, USA) using a Motor-driven Pellet Pestle (Polypropylene; Sigma), centrifuged at 13 000 r.p.m. for 5 min at 4°C. Supernatant samples were analysed for mouse tumour necrosis factor α (TNFα) and interleukin 1β (IL1β) using mouse specific antibody pair and protein standards developed for ELISA (enzyme-linked immunosorbent assay; R&D Systems, Abingdon, UK). For activated transforming growth factor β1 (TGFβ1) assay, a human specific antibody pair that cross reacts with mouse TGFβ1 was used (R&D Systems) as previously described (Cunningham *et al*., 2002). The detection limit for each cytokine was 31.2–2000 pg/ml with the recommended use of capture/detection antibody concentrations. As a positive control, serum from mice treated with lipopolysaccharide (20 μg/mouse i.v.; collection at 2 h and 24 h post-injection) was used. The colour reaction was read in a microplate reader at 450 nm, with absorbance at 540 nm taken as reference. Protein concentration was estimated using a bicinchoninic acid (BCA) protein assay (Pierce, Rockford, IL, USA). Cytokine levels were calculated as picogram of cytokine per milligram of protein.

In situ *detection of apoptotic cells (TUNEL)*

TUNEL (terminal deoxynucleotide transferase-mediated dUTP nick end labelling) staining was performed using the ApopTag Peroxidase In Situ Apoptosis Detection Kit (Oncor, USA) according to the manufacturer's instructions. Neonatal brain (day 5) sections were used as positive controls (data not shown).

Blood-brain barrier integrity

Integrity of the BBB was assessed using Evans blue extravasation (Murakami *et al*., 1997). Animals under anaesthesia were injected with 100 μl of Evans blue (4% in PBS) into the tail vein. Thirty minutes later mice were sacrificed by CO_2 asphyxiation, then immediately perfused through left cardiac ventricle with 60 ml heparinized saline to wash out any vascular Evans blue. Brains were removed, and each hemisphere was homogenized in 1 ml PBS and centrifuged at 1000*g* for 30 min. To the supernatants, an equal volume of trichloroacetic acid was added and incubated overnight at 4°C to precipitate protein. Following centrifugation at 1000*g* for 30 min, the extracted dye was diluted with ethanol (1:3) and its fluorescence was determined (Ex 620 nm and Em 680 nm) with a Jasco FP-777 spectrofluorimeter (Jasco UK Ltd, Essex, UK), and results were expressed as microgram per hemisphere.

Data analysis

Data are expressed as means ± SD. The statistical analysis of the data in Figs 6 and 8 was performed using the Student's *t*-test.

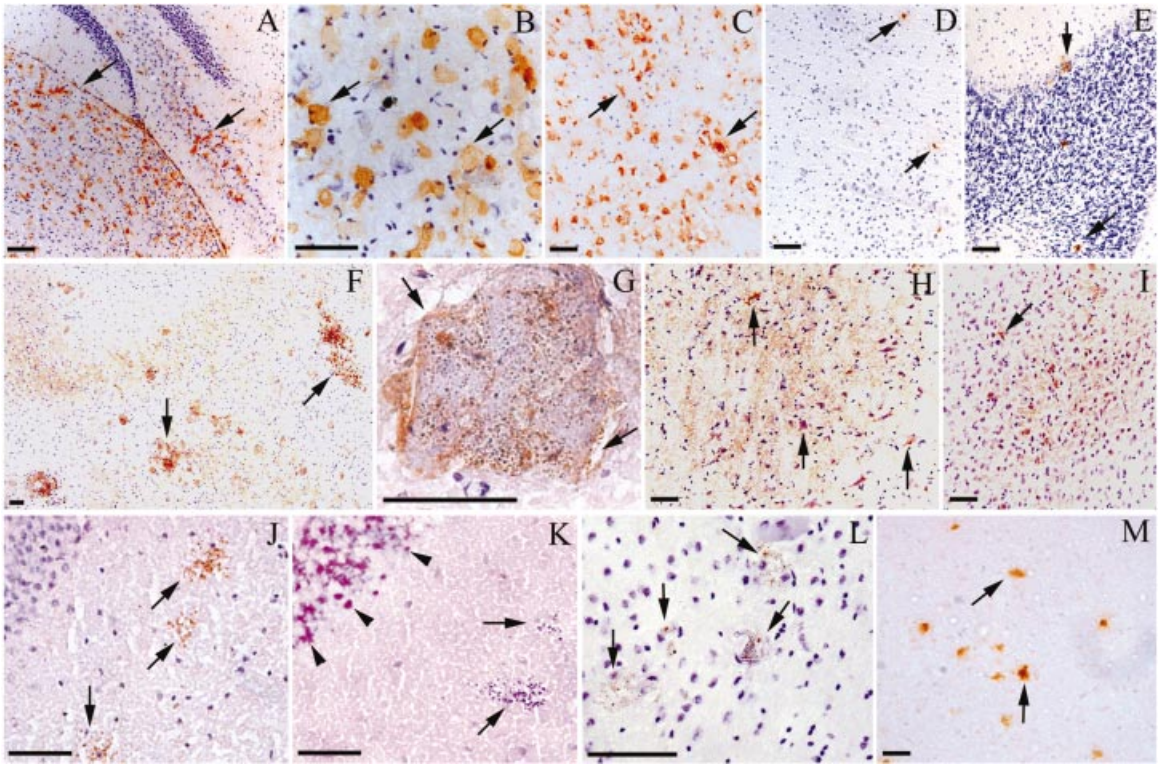

Fig. 2 (**A**–**M**) Representative light micrographs from mouse brain immunostained for MHC class II, TNF-R1 or Fas. Late disease stage brains are shown. MHC class II immunostaining in GM1 mouse hippocampus (**A**) and thalamus (**B**), Sandhoff mouse thalamus (**C**), LOTS mouse entorhinal cortex (**D**) and cerebellum (**E**). TNF-R1 immunostaining in GM1 mouse thalamus (**F** and **G**) and hippocampus (**J**), Sandhoff mouse brain stem (**H**) and LOTS mouse entorhinal cortex (**I**). (**K**) GM1 mouse brain stained for PAS to detect GSL storage. Arrowheads indicate CA1 field of hippocampus containing GSL storage. PAS+ fragmented cellular particles (arrows) also stain positive for TNF-R1 (arrows in **J**). Immunostaining of GM1 mouse thalamus for Fas (**L**) and Sandhoff mouse thalamus for CD8 (**M**). Scale bar = 16 μm.

Semi-quantitative grading of CNS inflammation

Immuno/lectin histochemistry was evaluated by grading the positive staining from 0 to 9+: scores 1+ to 6+ were based on the number of positive cells stained per section, and scores 7+ to 9+ were based on subjective scoring where cell counting was not possible due to very extensive staining. Specifically, 0 = undetectable; (1+) = 1–5 cells; (2+) = 6–15 cells; (3+) = 16–45 cells; (4+) = 46–150 cells; (5+) =, 156–300; (6+) = 301–500 cells; (7+) = abundant staining regionally; (8+) = abundant staining globally; and (9+) = global extensive staining. Comparable brain sections were selected for analysis. For analysing the spinal cord, cervical sections (C1–C3) were compared. These sections were independently evaluated by two investigators.

Results

Immunohistochemistry

To survey for inflammatory cells throughout the CNS, Tay-Sachs, LOTS, Sandhoff and GM1 gangliosidosis mouse models were analysed for inflammatory markers (Table 2) by immunocytochemistry. The data are summarized graphically in Fig. 1. MHC class II and TNF-R1 immunoreactivity was readily detectable in all the symptomatic mouse models examined (Fig. 1A; end-stage LOTS, Sandhoff and GM1 mice), but not in Tay-Sachs or wild-type mice (asymptomatic). Representative examples of immunostaining of mouse brain are shown in Fig. 2. In Sandhoff and GM1 mice, the microglial activation and/or Mϕ infiltrate was noted in virtually every region of the brain, although some regional variations in the staining intensity were evident. For example, staining for MHC class II was more pronounced in the thalamus and brain stem than in the cerebral cortex and hippocampus, both in Sandhoff and GM1 mice (Fig. 2A and B, GM1 mouse; Fig. 2C, Sandhoff). In the case of LOTS mice, MHC class II expression was only found in some parts of the brain such as lateral entorhinal cortex, cerebellum, hippocampus CA3 and caudate putamen (Fig. 2D and E).

Compared with MHC class II expression, only a subset of cells expressed TNF-R1, and these cells were found to be either clustered or scattered in the region of pathology (Fig. 2F and G, GM1 mouse; Fig. 2H, Sandhoff; Fig. 2I, LOTS). Furthermore, the topographical distribution and density of TNF-R1+ cells varied between disease models, with GM1 mice showing a stronger TNF-R1+ component compared with Sandhoff or LOTS mice (Fig. 2F–I). In brains of LOTS

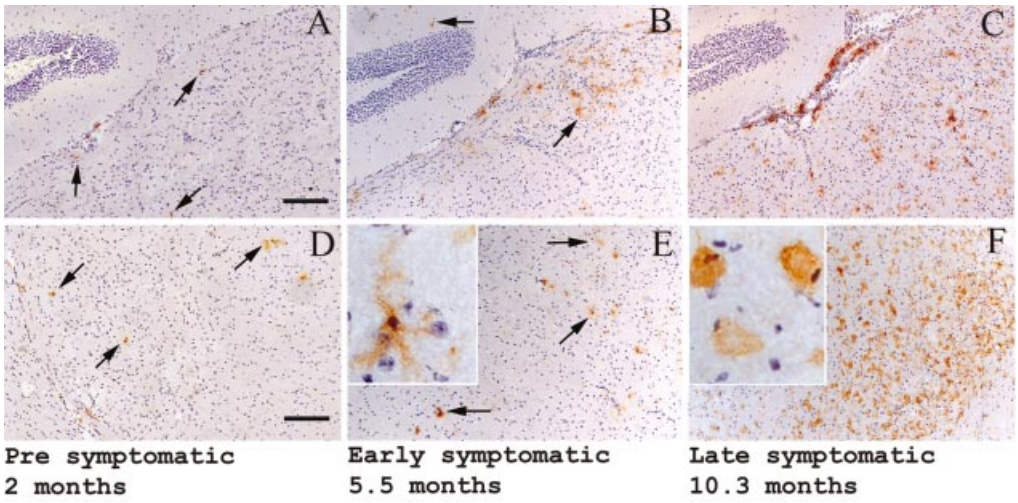

Fig. 3 Progressive increase in the number of MHC class II positive cells in the GM1 gangliosidosis mice. (**A**–**C**) hippocampus and dorsal thalamus; (**D**–**F**) ventral thalamus. Note that the majority of MHC class II positive cells at end-stage disease (**F**) appeared spherical with round cell bodies (**F**, insert) in contrast to the ramified phenotype in the early stages (**E**, insert). Scale bar = 200 μm.

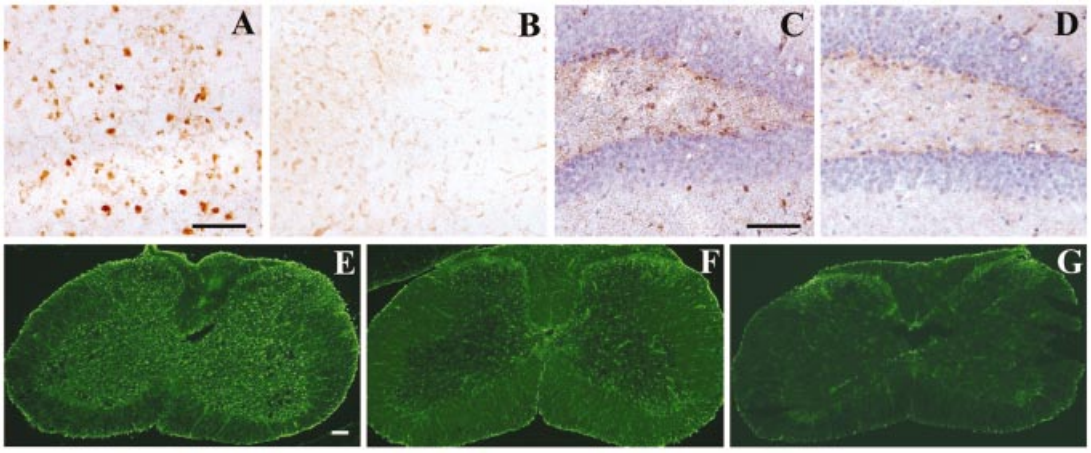

Fig. 4 Detection of microgliosis and astrogliosis in mouse brains. GSL I-B_4 lectin-stained thalamus from Sandhoff (**A**) and wild-type (**B**) mice. RCA_{120} lectin-stained hippocampus from Sandhoff (**C**) and wild-type (**D**) mice. GFAP immunostained spinal cord from Sandhoff (**E**), LOTS (**F**) and wild-type (**G**) mice. Scale bar = 50 μm.

mice, higher TNF-R1 expression was observed in the entorhinal cortex (Fig. 2I) compared with other cortical regions (not shown). Some of the TNF-R1+ components in GM1 mice brain appeared to have the morphology of fragmented cellular particles. Interestingly, these cellular particles, which are mainly found in the hippocampal formation (Fig. 2J), also stained positive for PAS (Fig. 2K, GSL storage product staining purple) and Fas (Fig. 2L).

Immunoreactivity to Fas was only detectable in GM1 mice at moderate levels and absent in all the other mouse models examined (Figs 1A and 2L). When immunostained with antibodies to CD68, CR3 (CD11b), 7/4 and F4/80, strong immunostaining was observed in the brain sections from the late-stage Sandhoff and GM1 mouse model [Fig. 1B, Sandhoff mice (GM1 mice not shown)]. When age-matched Tay-Sachs or wild-type mice were compared, weak immunostaining was noted for F4/80, CR3 (CD11b) and 7/4 antibodies within the brain parenchyma (Fig. 1B). As expected, no evidence of immune activation was evident within the brain parenchyma in these asymptomatic mice.

Immunostaining for T-cell subtypes using antibodies against CD4 and CD8 markers showed additional immunostaining of infiltrating cells in both Sandhoff and GM1 brains [Figs 1B and 2M, Sandhoff mice (GM1 mice not shown)]. Lymphocyte infiltrates only consisted of CD8+ cells restricted mainly to the thalamus (Fig. 2M, Sandhoff mice). These cells were either not present or very rare in wild-type, Tay-Sachs and LOTS mice.

To determine whether CNS inflammation in mouse models pre-dated symptom onset, a series of brain sections, from the level of the optic chiasma to mid cerebellum at various clinical stages were immunostained with antibodies specific for MHC

class II (Figs 1C and 2C, Sandhoff mice; Fig. 3, GM1 mice). In the thalamus of Sandhoff mice, MHC class II immunostaining was detected at a low level at 8 weeks of age and then gradually increased with age, leading to extensive staining in the later or terminal stages (Fig. 1C). The same phenomenon was observed in the brain stem, but staining was only detected from 12 weeks of age, with higher levels of staining than those seen in the thalamus (Fig. 1C). Interestingly, in other regions such as the cerebral cortex, hippocampus and cerebellum, the microglial activation and/or Mϕ infiltrate was found to be low with respect to thalamus and brain stem up to 14 weeks of age, and only became evident towards the terminal stage of the disease (Fig. 1C). This characteristic of progressive microglial activation and/or Mϕ infiltrate in Sandhoff mice was also seen with other immunological markers, such as CD68 and 7/4 (data not shown).

In the GM1 mouse brain the spatial distribution and extent of MHC class II immunostaining increased progressively over the lifespan and was detectable as early as at 2 months of age (Fig. 3A and D). MHC class II immunostaining was initially observed in the lateralposterier thalamic and lateral genuculate nuclei, extending at later stages to the other regions of the brain including cerebral cortex and hippocampus (Fig. 3). At the terminal stages, the majority of MHC class II positive cells appeared spherical with round cell bodies (Fig. 3F), in contrast to the ramified phenotype seen at early stages (Fig. 3E).

Lectin staining

Lectin staining (RCA_{120} and GSL I-B_4) was used to evaluate the morphology and activation state of microglia/Mϕ cells. The same spatio temporal patterns of microglia activation were observed in the different mouse models as were seen using microglia/Mϕ-specific antibodies. (Fig. 1B, graph data; Fig. 4A–D, light micrographs).

Astrogliosis

In parallel with microgliosis, a marked astrogliosis also occurred in all brain regions and spinal cord throughout the disease course, as determined by GFAP (glial fibrillary acidic protein) immunostaining (Fig. 4E–G, spinal cord data for Sandhoff and LOTS; GM1 mouse model not shown but qualitatively similar to Sandhoff).

Nitrotyrosine and inducible nitric oxide synthase enzyme distribution

Using immunohistochemical procedures, NITT (nitrotyrosine) and iNOS (inducible nitric oxide synthase) were found in all the symptomatic mouse brains and were evident throughout the late disease course, but were absent from the wild-type and Tay-Sachs mice (Fig. 5). NITT staining is a footprint of peroxynitrite (ONOO-) formation, a powerful oxidant and cytotoxic agent. iNOS immunoreactivity was found only in a subset of NITT+ cells (Fig. 5C and D). To determine the cell types labelled NITT+ or iNOS+, we double-immunostained with cell type specific markers such as CD68 (microglial/Mϕ), GFAP (astrocytes) and neurones (NeuN). Microglial/Mϕ cells appeared to contain higher levels of both NITT and iNOS signal than any other cell types (data not shown). The extent of NITT staining varied among disease models, but in general the trend was GM1 mice > Sandhoff mice > LOTS mice.

Cytokine production

Cytokines such as TNFα and IL1β are involved in the induction of acute inflammatory events and the transition to/persistence of chronic inflammation. To quantify the level of inflammatory cytokines (TNFα, IL1β and TGFβ1), ELISA assays were performed on whole brain homogenates. Of the three symptomatic animal models analysed, only Sandhoff and GM1 mice revealed an elevated level of cytokine production in their brains at the terminal stage (Fig. 6A). Sandhoff brain had ×3.6, ×2.8 and ×2.5 increases in TNFα, IL1β and TGFβ1 production, respectively ($P < 0.001$). For GM1 brain this was ×1.5, ×1.6 and ×1.25 ($P < 0.001$), and for the LOTS mice the values were comparable to wild-type and Tay-Sachs mice.

Interestingly, when SH-BMT (~ 18 weeks) and SH-NB-DNJ (~ 17 weeks) brains were analysed, they were found to have normal cytokine production, similar to wild type mice (Fig. 6A). This is in keeping with the reduction of storage and inflammation in the treated mice (Fig. 9).

When brains of Sandhoff mice at different clinical stages were analysed, increased production of TNFα and IL1β was noted in an age-dependant manner (Fig. 6B). Cytokines were first elevated in week 8 during the early symptomatic stage, and then gradually increased to the maximum levels towards the terminal disease phase. Compared with age-matched controls, only mice with severe/terminal disease, but not at earlier disease stages, had higher TGFβ1 levels in the brain ($P < 0.01$) (Fig. 6B). In addition to the brain tissues, circulating cytokines were also measured in Sandhoff mice at different age points. None of the cytokines analysed showed any significant changes with age and the values were comparable to the levels found in the wild-type serum (data not shown).

Apoptotic cell death in the CNS

Apoptotic cell death was determined by TUNEL staining. Brain and spinal cord sections from Sandhoff, GM1, LOTS and Tay-Sachs mice at different age points were compared. TUNEL+ cells were mainly detected in the terminal or late symptomatic stages of the animals (Fig. 7). During pre- or symptomatic stages, very few cells were stained by TUNEL. During later stages the number of cells labelled by TUNEL increased significantly in all symptomatic models, but in GM1 mice the number of TUNEL+ cells was much more

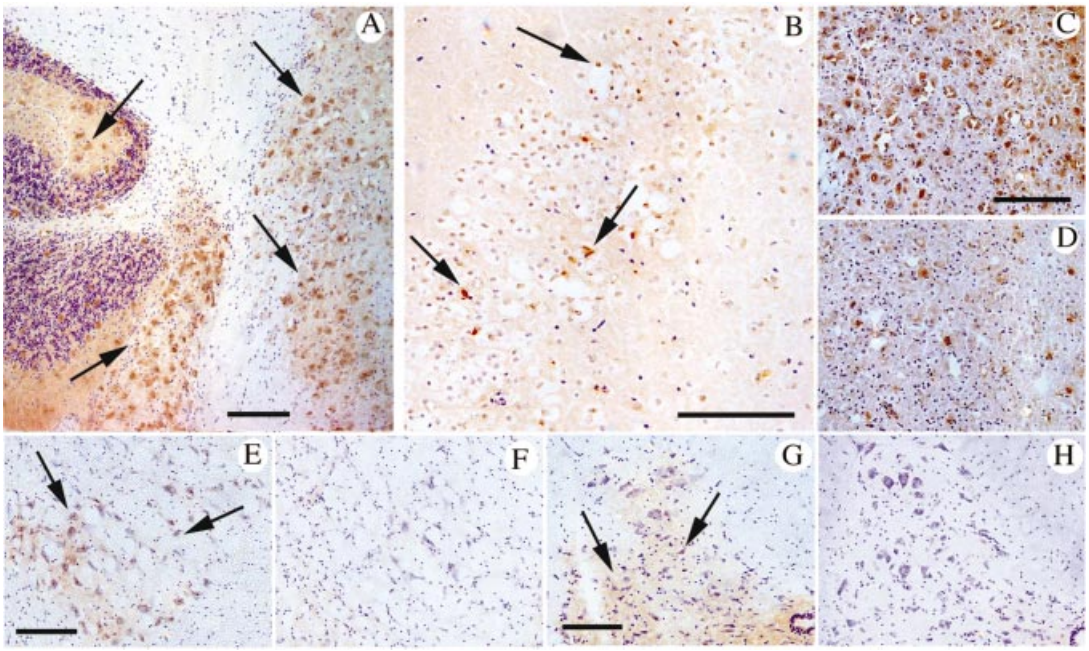

Fig. 5 Immunocytochemical detection of NITT and iNOS in mouse brains with GSL storage diseases. Late disease stage brains are shown. NITT immunostaining from GM1 mouse cerebellum-brain stem (**A**) and Sandhoff mouse cerebral cortex (**B**). (**C** and **D**) The midbrain dorsal raphe nucleus of GM1 mouse immunostained for NITT (**C**) and iNOS (**D**). (**E** and **F**) NITT immunostained magnocellular red nucleus of 18-month-old LOTS (**E**) and Tay-Sachs mice (**F**). (**G** and **H**) NITT immunostained cervical spinal cord of 18-month-old LOTS (**G**) and Tay-Sachs mice (**H**). Scale bar = 100 μm.

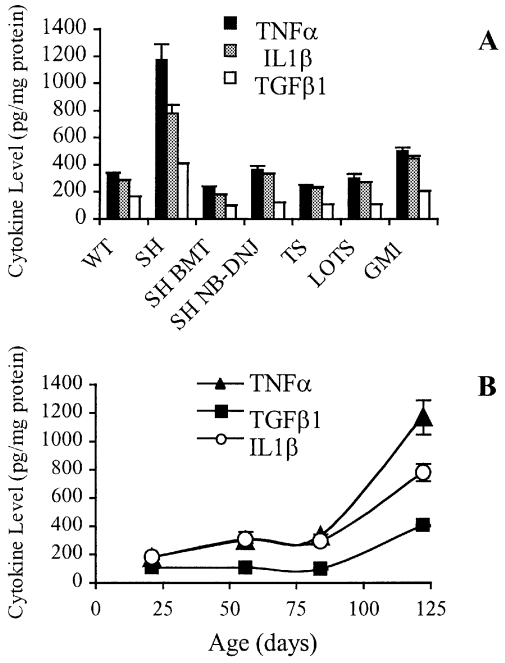

Fig. 6 Cytokine levels in brain (**A**) measured by ELISA in Sandhoff untreated (SH, ~17 weeks), Sandhoff BMT treated (SH BMT, ~18 weeks), Sandhoff *N*B-DNJ treated (SH-*N*B-DNJ, ~17 weeks), Tay-Sachs (TS, ~17 weeks), late onset Tay-Sachs (LOTS, ~20 months) and GM1 gangliosidosis mice (GM1, ~8.7 months). (**B**) Brain concentration of cytokine levels in Sandhoff mice at various age points. Data are mean ± SD of the values based on three to four animals in each group.

pronounced compared with Sandhoff mice. For example, in the cerebral cortex there was three-fold difference between Sandhoff and GM1 mice with respect to TUNEL staining. Furthermore, it was noted that in GM1 brains, the number of foam cells (large storage laden cells) that were TUNEL+ was greater than in Sandhoff brains (Fig. 7C and D), and a subset of these cells also stained positive for antibodies specific to TNF-R1 (Fig. 2F–J) and Fas (Fig. 2L). Both TNF-R1 and Fas are key mediators of inflammation-induced programmed cell death (Granville *et al*., 1998). TUNEL+ cells were also readily observed in the LOTS mice but were absent in the Tay-Sachs mice (Fig. 7G and H).

Blood-brain barrier integrity

BBB integrity was assessed by Evans blue extravasation and IgG immunohistochemistry (Fig. 8). Evans blue and IgG are normally excluded from the brain parenchyma by the BBB and are only detectable when the permeability of the BBB is increased. Altered BBB permeability was evident in Sandhoff and GM1 mice, but not in LOTS mice (Fig. 8A). During early- and late-symptomatic stages of Sandhoff disease, Evans blue content (μg/hemisphere) was significantly elevated from a control value of 0.149 ± 0.02 (n = 4) to 0.62 ± 0.03 (13 weeks, n = 6; $P < 0.031$) and 0.87 ± 0.35 (17 weeks, n = 3; $P < 0.0054$). Increased Evans blue content was also found in GM1 mouse brain with 0.59 ± 0.02 μg/hemisphere at 6.4 months (n = 3; $P < 0.0006$) and 1.02 ± 0.04 μg/hemisphere

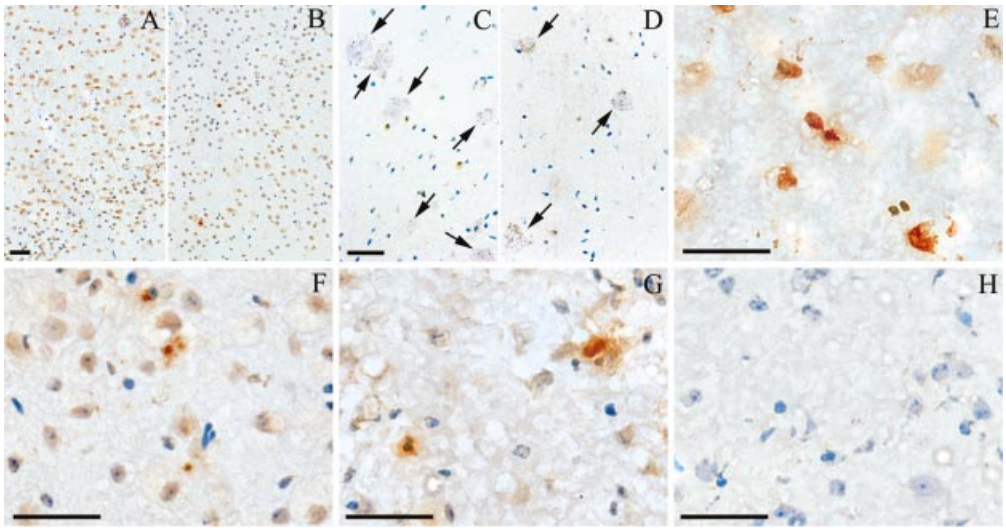

Fig. 7 Detection of apoptosis by DNA *in situ* end-labelling technique (TUNEL) in mouse brains. Late-stage frontal cerebral cortex of GM1 mouse (**A**) and Sandhoff mouse (**B**). Late-stage hippocampus of GM1 mouse (**C**) and Sandhoff mouse (**D**). Late-stage brain stem of Sandhoff mouse (**E**) and frontal cortex of GM1 mouse (**F**). Lateral entorhinal cortex of 18-month-old LOTS (**G**) and Tay-Sachs (**H**) mice. Scale bars = 100 μm.

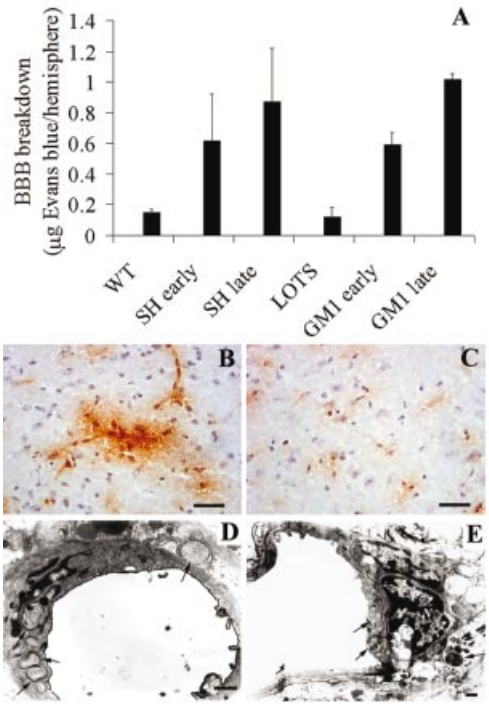

Fig. 8 (**A**) Extravasated Evan's blue content in mouse hemisphere. Data are mean ± SD of the values based on three to six animals in each group. Detection of leakage of IgG into the brain parenchyma in Sandhoff (**B**) and wild-type control (**C**) mice at 17 weeks of age; scale bar = 12.5 μm. (**D** and **E**) Ultrastructural changes in Sandhoff BBB; scale bar = 0.5 μm. Endothelial cells of the blood vessels in the hippocampal region containing numerous large vacuoles including MCBs. For Sandhoff mice, early is 13 weeks and late is 17 weeks, and for GM1 mice early is 6.4 months and late is 8.5 months.

at 8.5 months ($n = 3$; $P < 0.00001$). In the case of LOTS mice, there was no extravasation of Evans blue compared with the control mice (Fig. 8A). IgG immunostaining from late-stage Sandhoff animals revealed a pattern of leaky vessels within the brain parenchyma in regions including the stratum radiatum of the hippocampus, medial thalamus and the inferior colliculus (Fig. 8B and C). At the ultra-structural level, in addition to the neuronal inclusions, storage inclusions were noted in the endothelial cells of the blood vessels of the brain (Fig. 8D and E). In some areas, blood vessel walls appeared to be partly disrupted, and the cytoplasm of the endothelial cells was oedematous and contained numerous large vacuoles, including membranous cytoplasmic bodies (MCB) (Fig. 8D and E).

Effect of N*B-DNJ treatment on the onset of CNS inflammation*

As previously described, *N*B-DNJ treatment of Sandhoff mice delays symptom onset, slows the rate of disease progression and increases life expectancy (Jeyakumar *et al*., 1999). To determine whether *N*B-DNJ treatment, in addition to reducing neuronal storage, delays the onset of CNS immune activation, a series of brain and spinal cord sections of *N*B-DNJ-treated Sandhoff mice and untreated controls (17 weeks of age) were immunostained with antibodies to MHC class II and CD68 antigens (Fig. 9A–D). In the *N*B-DNJ treated mice, compared with untreated mice, the expression of MHC class II was reduced to background levels in the hippocampus, thalamus and cerebellum, whereas in the brain stem there was detectable staining, but still far less than in the

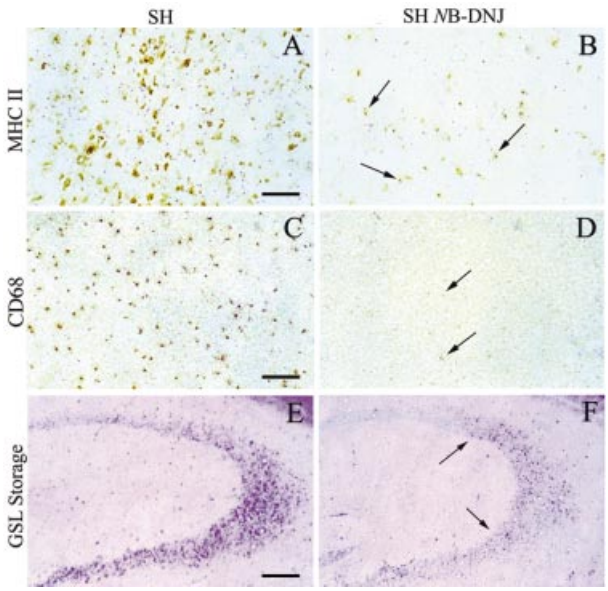

Fig. 9 Diminished expression of MHC class II and CD68 in Sandhoff mouse brain treated with *N*B-DNJ. Untreated (**A** and **C**) and *N*B-DNJ treated (**B** and **D**) mouse brain at 17 weeks of age (terminal stage for the untreated Sandhoff mice) (**A** and **B**, thalamus; **C** and **D**, cerebral cortex). PAS-stained brain sections of the untreated (**E**) and *N*B-DNJ-treated (**F**) Sandhoff mice at a similar age point. Arrows in the *N*B-DNJ-treated brain (**E**) indicate the reduction of PAS-positive neuronal inclusions and/or neuronal processes compared with the untreated brain. Scale bar = 50 μm.

untreated controls (Figs. 9A and B, thalamus; others not shown). Similar to MHC class II staining, the intracellular antigen CD68 expression was most pronounced in the untreated cerebral cortex, thalamus and cerebellum, and was completely absent in the *N*B-DNJ-treated mice (Fig. 9C and D, cerebral cortex; others not shown). In keeping with the previously published data (Jeyakumar *et al*., 1999), there was also a marked reduction of PAS-positive GSL storage in many areas of the brain and spinal cord (Fig. 9E and F, hippocampus; spinal cord not shown) due to *N*B-DNJ inhibiting GSL biosynthesis.

Discussion

In this study, we have demonstrated that inflammation, characterized by activation of cells of the Mϕ lineage, correlates with the disease severity in the gangliosidoses, irrespective of whether the storage ganglioside is GM1 or GM2.

Correlation of CNS inflammation with disease progression

In the mouse models of GM2 gangliosidoses, there was a correlation between inflammation and disease severity. Inflammation was absent in Tay-Sachs mice (asymptomatic) and readily detectable in LOTS mice (chronic disease), but was most extensive in Sandhoff (acute disease) and GM1 gangliosidosis mice. The pattern of tissue pathology and lipid storage correlated with the pattern of inflammatory marker expression, indicating that inflammation is predominantly confined to storage regions of the brain irrespective of the ganglioside species stored. In both the GM1 and GM2 gangliosidosis mouse models, the extent of inflammation correlated with disease progression with an age-dependent increase in microglial activation/Mϕ infiltration being observed. Significantly, this pre-dated the onset of overt clinical signs and became more extensive as disease progressed.

MHC class II is rarely expressed in healthy brain tissue, but is heavily expressed by microglial cells following inflammatory stimuli or during neurodegenerative processes such as those seen with Alzheimer's disease (Itagaki *et al*., 1988; Martiney *et al*., 1998; Perry *et al*., 1998). The enhanced MHC class II expression and the induction of lectin binding sites in the brain of Sandhoff, LOTS and GM1 mice results from microglial activation in the absence of foreign antigen. Extensive nitrotyrosine staining of macrophages, a footprint of nitric oxide (NO) formation, was observed, consistent with macrophage activation causing oxidative damage. In addition, nitrotyrosine staining was also observed in neurones, albeit at reduced intensity. NO is involved in important physiological functions within the CNS, including neurotransmission, memory and synaptic plasticity (Dawson and Dawson, 1998; Strijbos, 1998). Depending on the redox state of NO, it can act as a neurotoxin or it can mediate neuroprotective functions (Dawson and Dawson, 1998; Strijbos, 1998). Excessive production of NO following a pathological insult can lead to neurotoxicity (Dawson and Dawson, 1998; Strijbos, 1998). Data suggest that NO may play a role in the pathogenesis of neurodegenerative disorders such as Parkinson's disease, Alzheimer's disease and Huntington's disease (Dawson and Dawson, 1998; de la Monte *et al*., 2000; Barthwal *et al*., 2001). The gangliosidoses therefore represent another family of neurological disorders in which NO is implicated in their pathogenesis.

Cytokines in disease pathogenesis

At times of infection and inflammation, there is up-regulation of cytokines and their receptors within the CNS, with concomitant effects on brain function (McGeer *et al*., 1994). Cytokines produced by microglial cells, T-cells and macrophages determine the outcome of the inflammatory reaction. Interestingly, in the GSL storage mouse models, the observation that the microglial activation initially occurs in high storage areas such as the thalamus and brain stem indicates that once a critical threshold of storage is reached in that particular site, a signalling cascade may be triggered to activate microglial cells, which would in turn release inflammatory cytokines that amplify the inflammatory response by recruiting cells to that area. Accordingly, we have shown that the level of inflammatory cytokines (TNFα,

IL1β and TGFβ1) in Sandhoff and GM1 mice concomitantly rise as symptoms become more severe, suggesting that they are produced in response to, or contribute to, the local CNS immune activation. The cytokine levels correlated with the severity of the immune marker expression, such as MHC class II. Furthermore, increased production of TNFα and IL1β precedes clinical exacerbations in Sandhoff and GM1 mice, providing an insight into the temporal relationship between cytokine production and disease activity. Increased TNFα mRNA levels have also been reported in Sandhoff spinal cord by Wada *et al*. (2000), indicating that this is transcriptionally controlled up-regulation.

TGFβ1 was only elevated at the terminal stages of the disease in GM1 and Sandhoff mice, and could be a response to increased TNFα and IL1β throughout the disease course. TGFβ1 is an immunosuppressive cytokine, and acts by inhibiting TNFα, IL1, IL6 and IL12 production by microglia/macrophages (Martiney *et al*., 1998). Its expression is elevated in various diseases, including multiple sclerosis (Beck *et al*., 1991). During GSL storage pathogenesis, while the levels of TNFα and IL1β are progressively elevated throughout the disease course, TGFβ1 expression is only prominent during the later stages of disease. Considering the relatively late induction of TGFβ1, it is possible that TGFβ1 is produced in response to TNFα and ILlβ production to antagonize the effects of these pro-inflammatory cytokines. In this progressive disorder, this attempt at down-regulation of the inflammatory cascade is clearly too late to impact significantly upon the disease course.

Mechanism of CNS immune activation

At present, it is not known if the lysosomal storage *per se* or signals from the surrounding milieu triggers the observed microglial or Mϕ activation. One possible mechanism underlying microglial activation is binding and/or phagocytosis of apoptotic storage neurones by microglia. Normally, apoptotic cells are rapidly cleared without causing an inflammatory response (Fadok *et al*., 1998; Volbracht *et al*., 1999). This has been attributed to the rapid phagocytosis of apoptotic cells before cell lysis, thereby preventing the release of noxious contents that could provoke inflammation and tissue damage. However, in the storage disease condition this process may be impaired due to storage lipid driving the cell down a pro-inflammatory route. After dying cells containing storage lipids have been engulfed, microglial/Mϕ may actively alter the production of inflammatory mediators such as cytokines, prostaglandins and NO, which may lead to local damage to the CNS as demonstrated by the appearance of TUNEL+ cells. Gangliosides have been reported to activate microglia directly to produce proinflammatory mediators, including NO and TNFα *in vitro* (Pyo *et al*., 1999). The intracellular signalling molecules such as mitogen-activated protein kinase (MAPK) and NFκ-B have been implicated in this mechanism of activation (Pyo *et al*., 1999). This raises the possibility that clearance of apoptotic neurones is an initiating event in pathogenesis. It is interesting to note that the closer histochemical analysis of TUNEL staining in brains from Sandhoff and GM1 mice showed large cellular aggregates or foam cells that were TUNEL+. Furthermore, the accumulation of GSL and intracellular expression of TNF-R1 and Fas were also found in these cells. Apoptotic cell death may not be an inevitable fate of storage neurones, and other regional factors, inflammatory or intrinsic, may influence whether storage neurones survive or commit to apoptosis. If apoptosis is triggered by the storage lipid and initiates the disease process directly, it is clear from this study that this is not a unique property of GM2 storage, where neuronal apoptosis has been well documented (Huang *et al*., 1997; Wada *et al*., 2000), but also applies to the storage of GM1. It is important to note that in mice, due to sialidase activity in brain, appreciable storage of GA1 and GA2 occur in the GM1 and Sandhoff mouse models, respectively. To what extent these asialo derivatives of the primary storage lipids contribute to pathology in the mouse is not known.

The blood-brain barrier

In Sandhoff and GM1 mice, brain storage and/or CNS immune activation also induced a significant increase in BBB permeability, as evidenced by Evans blue extravasations. Initial increase in BBB permeability coincided with the onset of the clinical signs and microglial activation in the mouse models. Furthermore, in Sandhoff mice, there was a correlation between the level of pro-inflammatory cytokines in the CNS and BBB permeability. The pro-inflammatory cytokines IL1β and TNFα have also been shown to increase BBB permeability via cell recruitment (Anthony *et al*., 1997), suggesting that inflammation in the CNS acts to increase BBB permeability locally. Cellular inflammation may be initiated by the stored GSLs at the blood–microvascular endothelial cell interface observed in the Sandhoff mice. Whether the loss of integrity of the BBB is an essential step in the progression of the pathogenic process remains to be determined. However, in the LOTS mouse there was no detectable elevation in brain cytokine levels and no BBB breakdown, but there was microglial/Mϕ activation, apoptosis and oxidative damage. These data suggest that loss of BBB integrity is not a pre-requisite for disease onset or progression.

Treatment, neuropathology and inflammation

It has been reported previously that both BMT (Norflus *et al*., 1998) and SRT (Jeyakumar *et al*., 1999, 2001) show efficacy in the Sandhoff mouse model. If neuro-inflammation is a key player in the pathogenic process, effective therapies would be predicted to impact this process and delay inflammation. For instance, in the Sandhoff mice treated with BMT, life span was increased and neurological improvement demonstrated (Norflus *et al*., 1998). It is likely that enzyme-competent cells infiltrating the brain from the transplant are able to clear

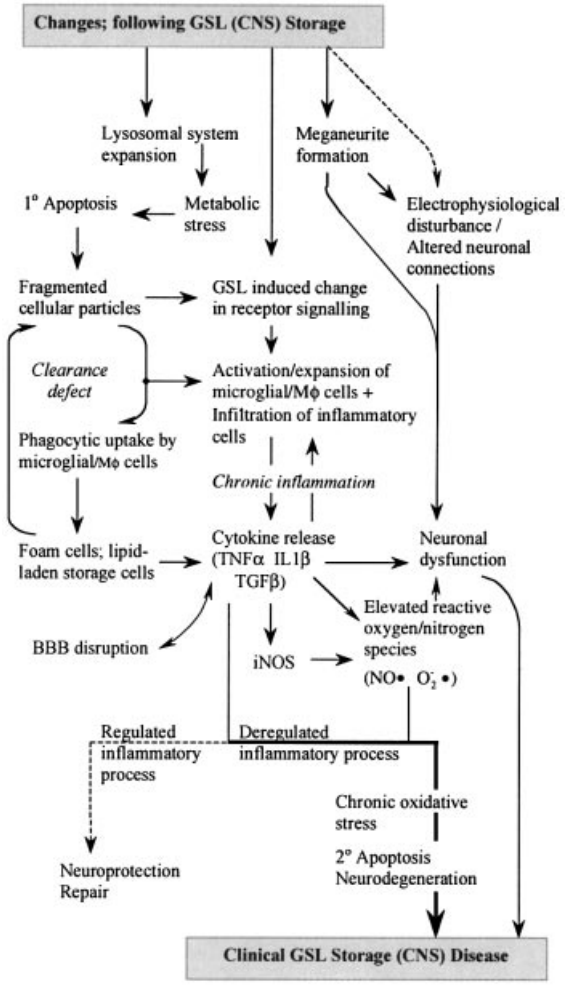

Fig. 10 Schematic showing the possible relationships of CNS GSL storage, pathogenic mechanisms and clinical signs. GSL-induced changes in the lysosomal system of neurones lead to stress responses leading to primary (1°) apoptosis of vulnerable neurones. Pathogenic phagocytic clearance leads to chronic inflammation involving elevated cytokine production and reactive oxygen/nitrogen species. Compromised BBB induced via cell recruitment further amplifies inflammation and promotes a chronic oxidative stress, leading to secondary (2°) apoptosis and neurodegeneration. Storage-induced meganeurites may also contribute further to neuronal dysfunction, possibly involving changes in electrophysiology and altered neuronal connections.

storage neurones dying by necrosis or apoptosis without leading to further macrophage recruitment, preventing the inflammatory process in the CNS (Norflus *et al*., 1998; Oya *et al*., 2000; Wada *et al*., 2000; Jeyakumar *et al*., 2002*a*). It was therefore of interest to see if the other proven therapy of Sandhoff mice, which has a different mode of action (without a cell replacement component), would also prevent inflammation in the CNS. We therefore evaluated the imino sugar inhibitor of GSL biosynthesis, *N*B-DNJ (Jeyakumar *et al*., 2001). When the brain and spinal cords of *N*B-DNJ-treated Sandhoff mice were examined it was found that, in addition to a reduction in GSL storage, the extent of inflammation, featuring microglial activation and/or Mϕ infiltration, was significantly reduced compared with untreated age-matched controls. This suggests that the level of neuronal storage can influence the kinetics of immune activation in the CNS.

Similarities to other neurodegenerative diseases

Microglial activation is also observed in many chronic neurological diseases including Alzheimer's disease, Parkinson's disease, amyotrophic lateral sclerosis (ALS), Huntington's disease and prion diseases (Kawamata *et al*., 1992; McGeer *et al*., 1994; Dawson and Dawson, 1998; Martiney *et al*., 1998; Perry *et al*., 1998; de la Monte *et al*., 2000; Barthwal *et al*., 2001). Inflammatory components of the CNS are suggested to play an important part in the pathophysiology of these diseases, although direct evidence is still lacking.

Activated cells generate oxygen-free radicals, NO and other potential toxins such as the cytokines IL-1β, IL-6 and TNFα. The activated microglia may contribute to neuronal dysfunction through secretion of these neurotoxic agents, which increase glutamate receptor-mediated excitotoxicity (Giulian, 1995). The phagocytic cells can also produce complement proteins that attach to their targets using surface receptors for immunoglobulins and complement components.

Studies in a murine model of prion disease have revealed that microglial activation is an early event that increases with disease progression, as indicated by the up-regulation of CD68 (Williams *et al*., 1994; Betmouni *et al*., 1996). In the twitcher mouse (Krabbe's disease model), elevated TNFα and MHC class II expression has been shown to contribute to the pathogenic course (LeVine and Brown, 1997), and in the SOD1 transgenic mouse model of ALS, evidence for peroxynitrite-mediated oxidative damage has been demonstrated in the brain (Cha *et al*., 2000). When twitcher mice were bone-marrow transplanted, improved survival was achieved with a down-regulation of several inflammatory mediators including cytokines and chemokines (Wu *et al*., 2001). In the Alzheimer's disease transgenic mouse model (APP Tg2576), CNS-derived cytokines IL-12 and IFNγ have been implicated in early disease development in parallel with microglial activation related to β-amyloid formation (Abbas *et al*., 2002).

Conclusion

The gangliosidoses are members of a growing family of neurodegenerative diseases triggered by unique biochemical processes, but which share a common neuroinflammatory response (Fig. 10). The fundamental question is whether inflammation is a critical factor in pathogenesis/disease progression or simply a common response to the primary disease processes. As shown in Fig. 10, there are numerous components to disease pathogenesis. We currently do not understand the relative significance of these pathways in disease initiation and progression. Our data from the mouse

models of GM1 and GM2 gangliosidosis are consistent with microglia/Mϕ activation playing a central role in the pathological process. It is therefore possible that anti-inflammatory drugs might be an effective form of therapy for the gangliosidoses either alone (chronic disease variants) or in combination (acute disease variants) with other proven therapies such as SRT (Jeyakumar *et al*., 1999, 2001) and BMT (Norflus *et al*., 1998).

Acknowledgements

We wish to thank Dr Donatienne Blond for aiding with ELISA methods and Liz Darley for cutting the brain sections. M.J. is supported by The Welcome Trust, and F.M.P. is a Lister Institute Research Fellow.

References

Abbas N, Bednar I, Mix E, Marie S, Paterson D, Ljungberg A, et al. Up-regulation of the inflammatory cytokines IFN-gamma and IL-12 and down-regulation of IL-4 in cerebral cortex regions of APP(SWE) transgenic mice. J Neuroimmunol 2002; 126: 50–7.

Anthony DC, Bolton SJ, Fearn S, Perry VH. Age-related effects of interleukin-1 beta on polymorphonuclear neutrophil-dependent increases in blood-brain barrier permeability in rats. Brain 1997; 120: 435–44.

Barthwal MK, Srivastava N, Dikshit M. Role of nitric oxide in a progressive neurodegeneration model of Parkinson's disease in the rat. Redox Rep 2001; 6: 297–302.

Beck J, Rondot P, Jullien P, Wietzerbin J, Lawrence DA. TGF-beta-like activity produced during regression of exacerbations in multiple sclerosis. Acta Neurol Scand 1991; 84: 452–5.

Betmouni S, Perry VH, Gordon JL. Evidence for an early inflammatory response in the central nervous system of mice with scrapie. Neuroscience 1996; 74: 1–5.

Cha CI, Chung YH, Shin CM, Shin DH, Kim YS, Gurney ME, et al. Immunocytochemical study on the distribution of nitrotyrosine in the brain of the transgenic mice expressing a human Cu/Zn SOD mutation. Brain Res 2000; 853: 156–61.

Cunningham C, Boche D, Perry VH. Transforming growth factor beta1, the dominant cytokine in murine prion disease: influence on inflammatory cytokine synthesis and alteration of vascular extracellular matrix. Neuropathol Appl Neurobiol 2002; 28: 107–19.

Dawson VL, Dawson TM. Nitric oxide in neurodegeneration. Prog Brain Res 1998; 118: 215–29.

de la Monte SM, Lu BX, Sohn YK, Etienne D, Kraft J, Ganju N, et al. Aberrant expression of nitric oxide synthase III in Alzheimer's disease: relevance to cerebral vasculopathy and neurodegeneration. Neurobiol Aging 2000; 21: 309–19.

Fadok VA, Bratton DL, Konowal A, Freed PW, Westcott JY, Henson PM. Macrophages that have ingested apoptotic cells in vitro inhibit proinflammatory cytokine production through autocrine/paracrine mechanisms involving TGF-beta, PGE2, and PAF. J Clin Invest 1998; 101: 890–8.

Giulian D. Neuroglia. New York: Oxford Publishing; 1995.

Gordon S, Lawson L, Rabinowitz S, Crocker PR, Morris L, Perry VH. Antigen markers of macrophage differentiation in murine tissues. Curr Top Microbiol Immunol 1992; 181: 1–37.

Granville DJ, Carthy CM, Hunt DW, McManus BM. Apoptosis: molecular aspects of cell death and disease. Lab Invest 1998; 78: 893–913.

Hahn CN, del Pilar Martin M, Schroder M, Vanier MT, Hara Y, Suzuki K, et al. Generalized CNS disease and massive GM1-ganglioside accumulation in mice defective in lysosomal acid beta-galactosidase. Hum Mol Genet 1997; 6: 205–11.

Hsu SM, Raine L, Fanger H. Use of avidin-biotin-peroxidase complex (ABC) in immunoperoxidase techniques: a comparison between ABC and unlabeled antibody (PAP) procedures. J Histochem Cytochem 1981; 29: 577–80.

Huang JQ, Trasler JM, Igdoura S, Michaud J, Hanal N, Gravel RA. Apoptotic cell death in mouse models of GM2 gangliosidosis and observations on human Tay-Sachs and Sandhoff diseases. Hum Mol Genet 1997; 6: 1879–85.

Itagaki S, McGeer PL, Akiyama H. Presence of T-cytotoxic suppressor and leucocyte common antigen positive cells in Alzheimer's disease brain tissue. Neurosci Lett 1988; 91: 259–64.

Jeyakumar M, Butters TD, Cortina-Borja M, Hunnam V, Proia RL, Perry VH, et al. Delayed symptom onset and increased life expectancy in sandhoff disease mice treated with N-butyldeoxynojirimycin. Proc Natl Acad Sci USA 1999; 96: 6388–93.

Jeyakumar M, Norflus F, Tifft CJ, Cortina-Borja M, Butters TD, Proia RL, et al. Enhanced survival in Sandhoff disease mice receiving a combination of substrate deprivation therapy and bone marrow transplantation. Blood 2001; 97: 327–9.

Jeyakumar M, Butters TD, Dwek RA, Platt FM. Glycosphingolipid lysosomal storage diseases: therapy and pathogenesis. Neuropathol Appl Neurobiol 2002a; 28: 343–57.

Jeyakumar M, Smith D, Eliott-Smith E, Cortina-Borja M, Reinkensmeier G, Butters TD, *et al.* An inducible mouse model of late onset Tay-Sachs disease. Neurobiol Dis 2002b; 10: 201–10.

Kawamata T, Akiyama H, Yamada T, McGeer PL. Immunologic reactions in amyotrophic lateral sclerosis brain and spinal cord tissue. Am J Pathol 1992; 140: 691–707.

LeVine SM, Brown DC. IL-6 and TNFalpha expression in brains of twitcher, quaking and normal mice. J Neuroimmunol 1997; 73: 47–56.

Liu Y, Hoffmann A, Grinberg A, Westphal H, McDonald MP, Miller KM, et al. Mouse model of GM2 activator deficiency manifests cerebellar pathology and motor impairment. Proc Natl Acad Sci USA 1997; 94: 8138–43.

Mannoji H, Yeger H, Becker LE. A specific histochemical marker (lectin Ricinus communis agglutinin-1) for normal human microglia, and application to routine histopathology. Acta Neuropathol (Berl) 1986; 71: 341–3.

Martiney JA, Cuff C, Litwak M, Berman J, Brosnan CF. Cytokine-

induced inflammation in the central nervous system revisited. Neurochem Res 1998; 23: 349–59.

McGeer PL, Rogers J, McGeer EG. Neuroimmune mechanisms in Alzheimer disease pathogenesis. Alzheimer Dis Assoc Disord 1994; 8: 149–58.

McLean IW, Nakane PK. Periodate-lysine-paraformaldehyde fixative. A new fixation for immunoelectron microscopy. J Histochem Cytochem 1974; 22: 1077–83.

Murakami K, Kondo T, Sato S, Li Y, Chan PH. Occurrence of apoptosis following cold injury-induced brain edema in mice. Neuroscience 1997; 81: 231–7.

Norflus F, Tifft CJ, McDonald MP, Goldstein G, Crawley JN, Hoffmann A, et al. Bone marrow transplantation prolongs life span and ameliorates neurologic manifestations in Sandhoff disease mice. J Clin Invest 1998; 101: 1881–8.

Oya Y, Proia RL, Norflus F, Tifft CJ, Langaman C, Suzuki K. Distribution of enzyme-bearing cells in GM2 gangliosidosis mice: regionally specific pattern of cellular infiltration following bone marrow transplantation. Acta Neuropathol (Berl) 2000; 99: 161–8.

Perry VH, Hume DA, Gordon S. Immunohistochemical localization of macrophages and microglia in the adult and developing mouse brain. Neuroscience 1985; 15: 313–26.

Perry VH, Bolton SJ, Anthony DC, Betmouni S. The contribution of inflammation to acute and chronic neurodegeneration. Res Immunol 1998; 149: 721–5.

Phaneuf D, Wakamatsu N, Huang JQ, Borowski A, Peterson AC, Fortunato SR, et al. Dramatically different phenotypes in mouse models of human Tay-Sachs and Sandhoff diseases. Hum Mol Genet 1996; 5: 1–14.

Platt FM, Reinkensmeier G, Dwek RA, Butters TD. Extensive glycosphingolipid depletion in the liver and lymphoid organs of mice treated with N-butyldeoxynojirimycin. J Biol Chem 1997; 272: 19365–72.

Pyo H, Joe E, Jung S, Lee SH, Jou I. Gangliosides activate cultured rat brain microglia. J Biol Chem 1999; 274: 34584–9.

Sango K, Yamanaka S, Hoffmann A, Okuda Y, Grinberg A, Westphal H, et al. Mouse models of Tay-Sachs and Sandhoff diseases differ in neurologic phenotype and ganglioside metabolism. Nature Genet 1995; 11: 170–6.

Sango K, McDonald MP, Crawley JN, Mack ML, Tifft CJ, Skop E, et al. Mice lacking both subunits of lysosomal beta-hexosaminidase display gangliosidosis and mucopolysaccharidosis. Nature Genet 1996; 14: 348–52.

Strijbos PJ. Nitric oxide in cerebral ischemic neurodegeneration and excitotoxicity. Crit Rev Neurobiol 1998; 12: 223–43.

Suzuki K. Twenty five years of the 'psychosine hypothesis': a personal perspective of its history and present status. Neurochem Res 1998; 23: 251–9.

Suzuki K, Sango K, Proia RL, Langaman C. Mice deficient in all forms of lysosomal beta-hexosaminidase show mucopolysaccharidosis-like pathology. J Neuropathol Exp Neurol 1997; 56: 693–703.

Taniike M, Yamanaka S, Proia RL, Langaman C, Bone-Turrentine T, Suzuki K. Neuropathology of mice with targeted disruption of Hexa gene, a model of Tay-Sachs disease. Acta Neuropathol (Berl) 1995; 89: 296–304.

Tifft CJ, Proia RL. The beta-hexosaminidase deficiency disorders: development of a clinical paradigm in the mouse. Ann Med 1997; 29: 557–61.

Volbracht C, Leist M, Nicotera P. ATP controls neuronal apoptosis triggered by microtubule breakdown or potassium deprivation. Mol Med 1999; 5: 477–89.

Wada R, Tifft CJ, Proia RL. Microglial activation precedes acute neurodegeneration in Sandhoff disease and is suppressed by bone marrow transplantation. Proc Natl Acad Sci USA 2000; 97: 10954–9.

Walkley SU. Cellular pathology of lysosomal storage disorders. Brain Pathol 1998; 8: 175–93.

Williams AE, Lawson LJ, Perry VH, Fraser H. Characterization of the microglial response in murine scrapie. Neuropathol Appl Neurobiol 1994; 20: 47–55.

Wu YP, McMahon EJ, Matsuda J, Suzuki K, Matsushima GK. Expression of immune-related molecules is downregulated in twitcher mice following bone marrow transplantation. J Neuropathol Exp Neurol 2001; 60: 1062–74.

Yamanaka S, Johnson MD, Grinberg A, Westphal H, Crawley JN, Taniike M, et al. Targeted disruption of the Hexa gene results in mice with biochemical and pathologic features of Tay-Sachs disease. Proc Natl Acad Sci USA 1994; 91: 9975–9.

Received July 24, 2002. Revised November 11, 2002.
Accepted November 11, 2002